Novel Fluidized Bed Particle Classifier for Application in Calcium Looping With Indirect Heat Transfer – Experiments and Simulations

Article *in* SSRN Electronic Journal · January 2021

DOI: 10.2139/ssrn.3820682

CITATION
1

READS
29

3 authors:

Chameera Jayarathna
SINTEF
31 PUBLICATIONS **137** CITATIONS
SEE PROFILE

Britt M. E. Moldestad
University of South-Eastern Norway
75 PUBLICATIONS **264** CITATIONS
SEE PROFILE

Lars-André Tokheim
University of South-Eastern Norway
70 PUBLICATIONS **477** CITATIONS
SEE PROFILE

15th International Conference on Greenhouse Gas Control Technologies, GHGT-15

15th 18th March 2021 Abu Dhabi, UAE

Novel fluidized bed particle classifier for application in calcium looping with indirect heat transfer – Experiments and simulations

Chameera K. Jayarathna[a,b*], Britt E. Moldestad[b], Lars-André Tokheim[b]

[a]*SINTEF Tel-Tek, SINTEF Industry, P.O. Box 5, 3901, Porsgrunn, Norway*

[b]*University College of Southeast Norway, Faculty of Technology, Kjølnes ring 56, 3918, Porsgrunn, Norway*

Abstract

This article summarizes a detailed scientific study of a particle classification system to be used in a fully integrated regenerative calcium looping (FICaL) system for CO_2 capture. In conventional calcium looping, the required calcination heat is provided by a separate oxyfuel combustor, which needs an air separation unit (ASU) to provide the required oxygen for the process. The ASU demands a considerable amount of power, which gives an energy penalty of typically 5 % to the power plant. However, in the FICaL system, the required heat for the calcination is instead supplied indirectly from the main combustor in the power plant, so there is a no need for an ASU in the system. Based on process simulation studies done with Aspen Plus®, this may reduce the energy penalty to values in the order of 1-2 %. The indirect heat transfer is done by using inert heat transfer (HT) particles that are heated up in the combustor and then transferred to the calciner where the sorbent material is heated up after mixing with the hotter inert particles. Thereby the sorbent material is calcined. However, after calcination, the sorbent and heat transfer particles have to be separated. Hence, an efficient classifier is required. The current work has therefore focused on designing, constructing and doing experiments in a novel particle classification system.

A novel cross-flow fluidized bed classifier was designed, using computational fluid dynamics (CFD) simulations as a tool, in order to separate the sorbent and HT particles exiting from the calciner. The classifier, which has no mechanical moving parts exposed to very high temperature, can be operated under the required high-temperature conditions prevailing in a full-scale plant.

Two different cold-flow lab-scale versions of the classifier was built and used for a large number of experiments. In the classification, the aim is to minimize the loss of sorbent particles via the bottom exit from the classifier, and also to minimize the loss of HT particles via the top exit from the classifier. The second and improved version was able to classify very well a mixture of down-scaled sorbent particles (zirconia) and down-scaled HT particles (steel). The experiments with the improved classifier version gave particle losses in the order of 2-3 %, values that are close to what can be seen as acceptable in a full-scale hot-flow system.

Extensive CFD simulations were carried out with the commercial software Barracuda® 17.1 to investigate in detail how the different particle types behave in the classifier. Even if the exact particle losses were not well predicted, Barracuda was able to predict the general gas-solids flow behavior and proved to be a useful tool in the design process. Different drag models were used to reproduce the experimental findings and validate the CFD model. Barracuda was also used to simulate the classification process under hot-flow conditions and indicated that the classifier will also perform well under such conditions. The results of the corresponding research work are promising as the classifier is able to give a high degree of purity of the particle streams leaving the classifier. The iterative design and modelling effort from this research work has produced a functional, high-efficiency classification concept.

Keywords: Type your keywords here, separated by semicolons ; these should also be cut and pasted into the key words field on the upload full paper process

* Corresponding author. Tel.: +47 40325972, *E-mail address:* chameera.jayarathna@sintef.no

1. Introduction

Here Since greenhouse gas (GHG) emissions from human activities is a major cause for the global warming and the rise of average temperature of the earth's atmosphere and ocean, there is an urgent need to control those emissions for the sake of the future generations on earth. Just considering the last 100 years the average increment is 0.8ºC (1).

Deforestation and burning of fossil fuels are the two main human activities that release large amounts of GHG's to the environments. CO_2 lead the way as the most fearful GHG due to its vast production specially from burning coal, oil and natural gas and the production of cement. It was about 8.5 Gt carbon per year in 2007 (2) and the same figure was increased to 10Gt in 2014 (3). During the past 10 years, many political efforts have been made to force worldwide agreement to the Kyoto treaty (4) and then lately with the Paris agreement(5). According to the Paris agreement a significant reduction of CO_2 release to the environment is needed in order to keep the increase in global average temperature below 2 °C to reduce the risk of climate change due to global warming. Coal combustion for power generation is a major source of CO_2 emissions, but it is also a process suitable for different CO_2 capture technologies.

Post combustion CO_2 capture is not a very new idea, but the related technology is developed to a large extent during the last 10 years. Carbon capture from the flue gas of the coal power plant based on amine solutions is widely studied and the technology is matured enough to apply on power plants already (6-8). However, other concepts may be more attractive from an energy penalty point of view. Using a solid sorbent at elevated temperature is a concept which is now being considered as an alternative. Even though the carbon capture based on solids is not a new concept there are several major reasons which hold the development of this technology from behind, mainly lack of cheap and easy operational sorbents and the related technology (9). Development of more advanced solid sorbents is a continuous process, but a challenge is high sorbent production cost.

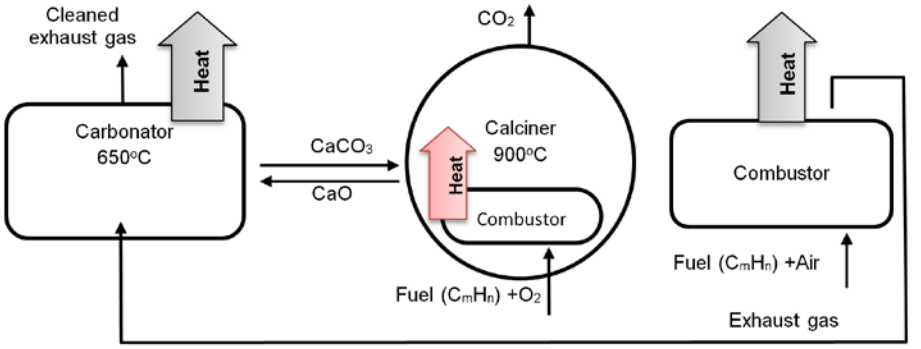

Fig. 1. Calcium looping cycle with direct heat transfer from the oxyfuel combustor placed inside the calciner

CO_2 capture from flue gas by carbonate looping may be an attractive alternative due to the cheap and readily available sorbent (limestone), but handling limestone as a sorbent is not an easy task due to very high calcination temperature. Calcium looping (CaL) is a promising CO_2 capture technology as it may considerably, reduce the energy penalty represented by the capture system (10).

In calcium looping, first described by Shimizu et al. in 1999 (11), calcium oxide (CaO) reacts with CO_2 to form calcium carbonate ($CaCO_3$) in a fluidized bed reactor (carbonator) at a temperature around 650 °C (the temperature being a trade-off between thermodynamics and kinetics). The $CaCO_3$ is then separated from the gas in a cyclone separator and passed on to another fluidized bed reactor (calciner) where the $CaCO_3$ decomposes into CaO and CO_2 at a temperature above 900 °C at thermodynamic equilibrium. The cleaned flue gas exiting from the carbonator can be released to the atmosphere. The regenerated CaO is separated from the CO_2 by another cyclone and recycled back to the carbonator, and the CO_2 is removed from the system. Since $CaCO_3$ is present in part of the system, the process is also called carbonate looping (12), or carbonate cycling.

The energy required for regenerating the sorbent originates from the combustion process in the boiler section of the power plant. CaL can be separated into two different categories based on how this regenerative energy (the heat required to heat up and decompose $CaCO_3$ into CaO and CO_2) is supplied to the calciner; directly or indirectly.

In the direct heat transfer system (see Fig. 1), the calcination heat is transferred by the internal oxyfuel combustor. Oxyfuel combustion is used in order to avoid adding nitrogen (from combustion air) to the CO_2 product. Several pilot

plants based on the direct heat transfer concept are in operation (13-17) around the world and the disadvantage here is the energy penalty introduced via the air separation unit (ASU), which reduces power plant efficiency by several percentage points (~5-7 points, without compression) (18).

If the calcination heat could be transferred directly from the main combustor in the system, the additional oxyfuel combustor and the air separation unit (ASU) could be avoided as described by Strelow et al. (19). In addition, the clean-up associated with CO_2 purification can also be avoided which allows for a considerable improvement in overall process efficiency (~1 percentage point loss, without compression). The fact that the heat transfer takes place at a temperature higher than the typical operational temperature of the steam cycle in a coal fired power plant means that the energy penalty usually associated with CO_2 capture processes can be significantly reduced. The low energy penalty of CaL with indirect heat transfer is due to the high-temperature integration between the CO_2 capture plant and the power plant (19, 20). The concept is illustrated in Fig. 2 (21), and may be called fully integrated calcium looping (FICaL).

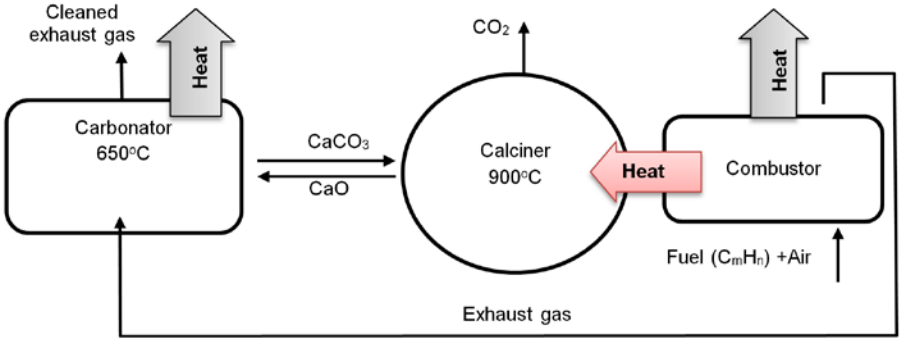

Fig. 2. Calcium looping cycle with indirect heat transfer between the combustor and the calciner(21)

The indirect heat transfer system in FICaL is challenging to design and develop due to the high temperature. Mechanical moving parts, such as pumps and fans, and sensitive process equipment units, such as filters, are vulnerable and should be avoided in the high temperature areas in the system. Probably some expensive materials can be used to design a classical heat exchanger in between main combustor and the calciner in the system. Even if the cost is neglected still the following heat exchanger could be susceptible to damages. Some research groups have investigated the possibility of heat transfer by means of heat pipes (22-26). Such systems consist of liquid/vapor cycling between the combustor (evaporation) and the calciner (condensation), but wear and potential leakages may be a challenge, in addition to high costs. The use of high temperature steam or recycled CO_2 as a heating medium could be a possibility (27), but high gas flow rates may be required, and it may be difficult to avoid local overheating and also to achieve a good gas distribution in the calciner. Using heated steam or CO_2 to transfer heat could be inefficient as heat would have to be transferred through several media before reaching the solid particles in the calciner. This is illustrated in Fig. 3.

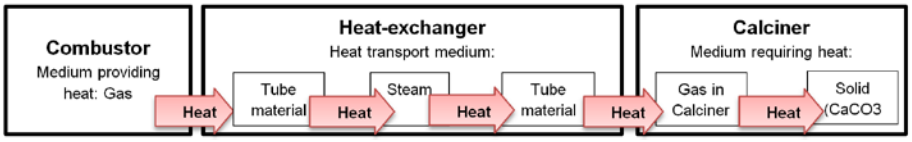

Fig. 3. Concept of indirect heat transfer from an external combustor to solids in the calciner by using steam

Another alternative is to use inert solid particles as a heat transfer medium. In such a scheme, which is shown in Fig. 4, the indirect heat transfer process is realized by combining two direct heat transfer processes: the first one being direct heating of inert particles by hot combustion gases in the combustor, the next one being heating of $CaCO_3$ particles by direct contact with the inert heat transfer particles in the calciner (28-30).

These possibilities are discussed and these alternative heat transfer mechanisms were studied further based on Aspen Plus® simulations (27, 31).

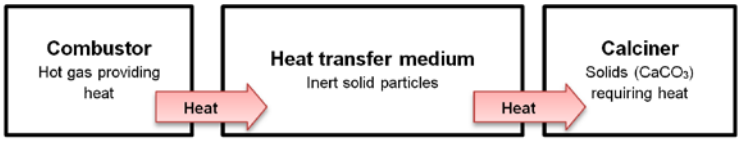

Fig. 4. Concept of indirect heat transfer from an external combustor to the calciner by means of inert solid particles

However, even if the solid-to-solid heat transfer concept may be a solution to the heat transfer problem, another challenge arises; that of separating the calcined particles from the inert solids after the calcination. Such a separation requires an efficient classification system. A novel solid classification system to separate a binary mixture particle with different size and density was designed based this requirement.

A coal fired power plant with a FICaL-based CO_2 capture facility was simulated using Aspen Plus V8.6® software. Several different indirect heat transfer cases were simulated and analyzed. The aim was to determine the impact on the energy balance of the system for each case. The capacity of the power plant was 1890 MW^{th}.

The Aspen Plus model contains all the main units in the process. Eight different case studied were done with the Aspen Plus® process simulation and results are published in two publications (27, 31). Based process simulations it is concluded that the FICaL can be categorized as an attractive technology with a low energy penalty when applied to a coal-fired power plant. Various concepts of indirect heat transfer were studied and evaluated through process simulations with Aspen Plus. Based on these studies, FICaL can be categorized as a competitive technology with a low energy penalty. A simplified method was used to estimate energy penalties in the order of 1 %.

2. Test facilities and experiments

It was decided to use inert solid particles (HT solid particles) to transfer the calcination heat from the main coal combustor to the calciner. The decision was based on the process simulations and a feasibility study done in the research work as well as a study related to risk, safety and maintenance of the heat transfer system which involved the other project participants (IFE, ETH and GE). In this concept, HT solids are heated in the combustor and then transferred to the calciner. These HT solids are then mixed with the sorbent particles in the calciner and transfer the heat directly due to the solid-to-solid contact.

As described in the Introduction, the new heat transfer concept required an efficient solid classification system which should be compatible with the operating conditions in the plant. The novel solid classification concept developed for the FICaL system is described here in detail.

The novel solid classifier is designed with the multistage cross-flow fluidization system, which is supposed separate a mixture of solid sorbent and HT particles. In a hot-flow system, this particle mixture consists of CaO particles as the solid sorbent and alumina particles as the HT solids.

Experimental investigation of the classification concept is very important. It gives an indication of the performance of the novel concept and a large amount of information which could be useful for improvements. However, building a classification rig operating under high temperature conditions is not practical at the initial stage. Because of that, it was decided to build a down-scaled version of the classifier rig operating under cold-flow conditions (room temperature). Down-scaling calculations were done based on the Glicksman scaling rules (32-34), the cold-flow system was designed to operate with zirconia-based beads representing the sorbent, steel shots representing the heat transfer solids (HT solids) and air at room temperature replacing the hot fluidization gas (CO_2) as these media were available and had characteristics relatively close to theoretical optimum values. Further information about the classification concept down-scaling calculations and the materials selections for the cold-flow conditions are reported in Jayarathna et al. (35).

The commercial CFD software Barracuda®, version 17.1, was used as supporting tool for the classifier design task. A considerable number of CFD simulations were done prior to the initial design of the novel solids classifier. The initial design that was built is named as version 3.0v in the current document (there were several designs prior to the 3.0v and those versions failed due to low classification efficiency and high air consumption).

Both in the experimental work and in the simulations, information about the fluidization characteristics of the particles was required. Basic fluidization experiments with increased and decreased air flow rates were done for both

particle types in a fluidized bed test rig. The possibility of separating a binary particle mixture with different size and density were initially tested in the same rig. These experiments were done prior to the fabrication of the new classifier.

2.1. Fluidized bed test facility and experiments

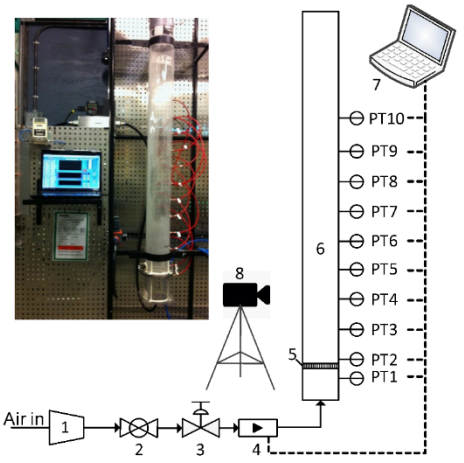

The fluidization test rig (see Fig. 5) is designed to work with two cylindrical beds with different diameters. The beds are made of Lexan plastics to enable visual observations of the flow behavior, and fluidization air is pumped into the bed from the bottom of the bed via an air distributor. A stainless-steel porous membrane R20, manufactured by Siperm GmbH, was used as the air distribution plate.

Pressure sensors are placed along the bed to measure the pressure drop during the experiments. The air flow for the fluidization is controlled by Sierra mass flow controllers. Pressure data are recorded using a LabVIEW® program. Further information on the test facility and experimental findings related to the current research work are reported in Chladek et al. (36), Jayarathna et al. (21), Amarasinghe et al. (37) and Jayarathna et al. (38).

Fig. 5. Fluidized bed experimental rig: 1 – compressor, 2 – ball valve, 3 – pressure regulator, 4 – mass flow controller, 5 – air distribution plate, 6 – fluidized bed column, 7 – DAQ and LabVIEW®, 8 – video camera

3. Solids classifier test facility

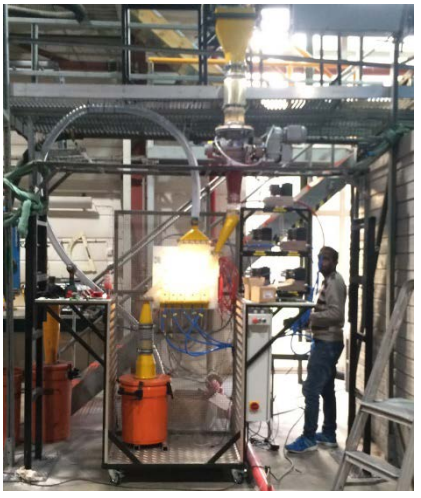

Fig. 6. Solids classification test facility

Solids classification test rig was designed with several equipment units in addition to the custom-made classifier and the metal frame on which all the equipment was mounted as shown in Fig. 6.

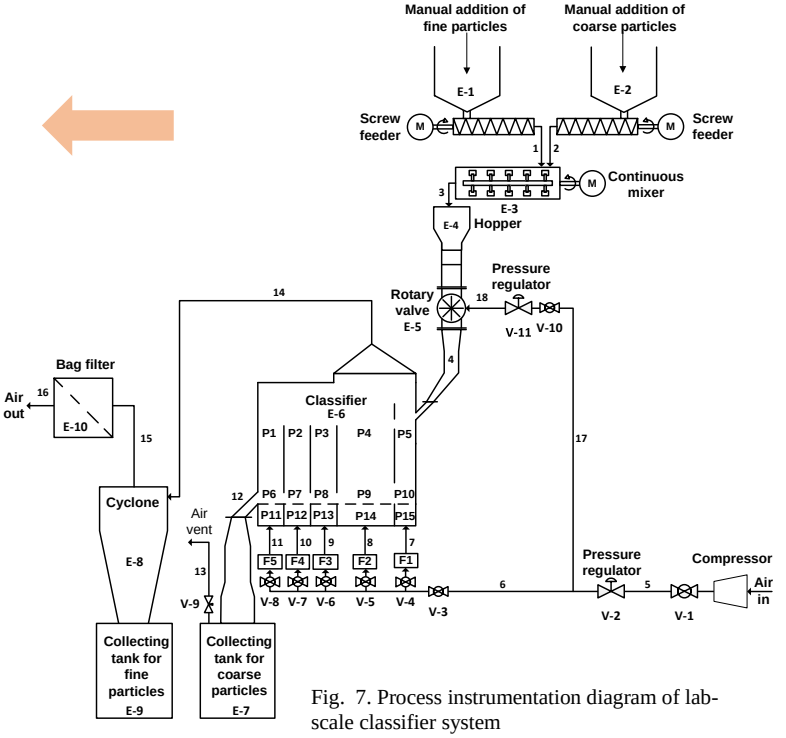

Fig. 7. Process instrumentation diagram of lab-scale classifier system

Set up is connected to a computer via LabVIEW® based control and data collection programme with the possibility of writing the pressure data and control the gas flow controllers. Process instrumentation diagram of lab-scale classifier system is shown in Fig. 7.

The two particle types are discharged from separate material tanks via two screw feeders (E-1 and E-2) and are then mixed in a rotary mixer (E-3). The mixture is fed to the classifier via an airtight rotary valve (E-5).

The most important part of the cold-flow lab rig is the classifier itself (E-6), see Figure 3-16. The classifier has five separate compartments divided by walls (see Fig. 7) so that air is fed to each parallel pass. Depending on the air velocity and particle characteristics each compartment functions as a separate bubbling fluidized bed or an entrainment bed or a combination of these two bed types. Solid particles are fluidized with fluidization air injected through a porous bottom plate in each of the fluidization compartments. The fluidization air is supplied by a compressor via a buffer tank and a pressure control valve (V-2). In this way, the air entrains fine solids from the dense zone into the freeboard zone, while the coarser and heavier particles remain in the dense bed.

The air velocity is gradually increased from compartment 1 to compartment 5, which allows smaller sorbent particles with lower terminal velocities to leave the classifier first and minimizes entrainment of fine HT solids particles. In the second compartment, bit coarser particles may be entrained, in the third compartment even coarser particles, and so on.

In a fluidized bed with entrainment, the freeboard zone is acting as the main classification region where lighter particles are entrained and where heavier particles change their direction and return to the dense bed (39). A high freeboard zone could increase the classification efficiency. According to Kunnii and Levenspiel (39), the bubbles and slugs breaking at the surface of the bed throw the solids into the freeboard. The walls between each compartment are limiting the diameter of the bubble created in the dense bed. Due to this, bubbles are forced to burst early, thus creating a freeboard zone a bit earlier than in a similar classifier without separate compartments. Detailed information about the experimental procedure and theoretical background of the design concept is reported in Jayarathna et al. (35) and further updates are included in Jayarathna et al. (40).

3.1. Classification compartment

Several versions of the classifier were studied based on CFD simulations: 1.0v, 2.0v, 4.1v, 4.2v, 4.3v, 4.4v, 4.5v, 5.0v and 5.1v. Version 1.0v was based on the fast fluidization concept, but a poor classification performance was found. The classifier versions after version 2.0V were based on the multistage cross-flow fluidization concept, and different features were tested to improve the classification performance. Version 3.0v (see Fig. 9) was the first version that was fabricated and used in cold-flow experiments. Based on the experimental studies done on version 3.0v and CFD simulation studies done on versions 4.0v to 5.1v, version 5.1v (see Fig. 8) was also fabricated and used in further cold-flow experiments.

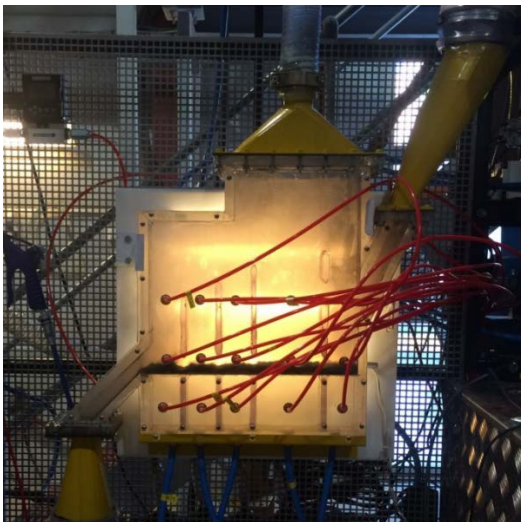

Fig. 9. The Plexiglass classifier unit 3.0v connected to solids and gas inlets and outlets and 15 pressure tappings, and equipped with a backlight to facilitate visual observation

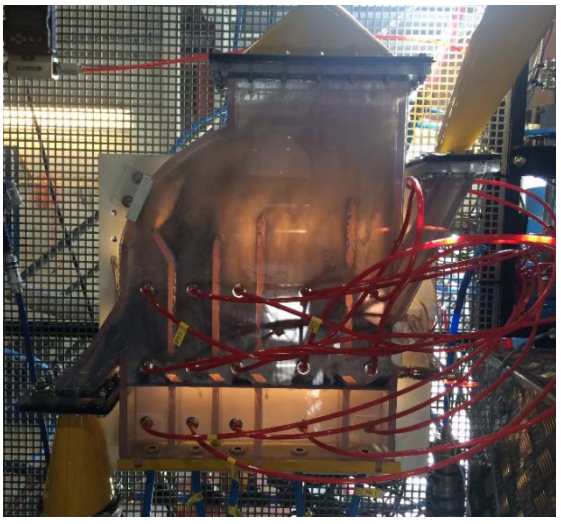

Fig. 8. The Plexiglass classifier unit 5.1v connected to solids and gas inlets and outlets and 15 pressure tappings, and equipped with a backlight.

A details investigation of the performances of the classifier 3.0v and 5.1v are reported in Jayarathna et al. (35) and Jayarathna et al. (40), respectively.

4. CFD simulations for cold-flow solids classification systems

The CFD tool Barracuda® 17.1 is extensively used during the development of FICaL solid classification system. This type of gas-particle CFD studies are also known as Computational Particle Fluid Dynamics (CPFD). CPFD (41) is a method developed based on a new Eulerian–Lagrangian multiphase flow scheme. It is also called as Multiphase-Particle-In-Cell (MP-PIC) (42) method. Their commercially developed platform known as Barracuda®, can be applied to much larger systems. Eulerian description is used to model the gas phase and it is approximated as a continuum and the velocity, temperature, and density fields are solved using the appropriate conservation and constitutive laws. The discrete Lagrangian approach is used to model the particle phase.

The averaged Navier–Stokes equations are used in the Barracuda CFD code to solve the fluid and particle equations in three dimensions. The inventor of the Barracuda CFD code, Professor Snider and his subordinates explained the strong coupling between the fluid and particles phases in their papers (41, 43). The specialty in Barracuda compared to the conventional DEM method is that Barracuda follows the concept called multi-phase particle-in-cell (MP-PIC) (42) formulation. The particle momentum equation uses the MP-PIC concept, including a relaxation-to-the-mean term to represent damping of particle velocity fluctuations due to particle collisions (41, 43). Through the computational particle concept, simulation of large industrial fluidized-bed reactors is possible.

Designing a novel classification concept for a hot flow system could be time consuming uneconomical task without the CFD studies.

Several simulations were done to study the fluidization characteristics of the particles in the bubbling fluidized bed. These simulations were done with a cylindrical geometry at cold-flow conditions. Chladek et al. (36), Jayarathna et al. (21), Amarasinghe et al. (37) and Jayarathna et al. (38) are published based on the pure solid and solid mixtures fluidization studies and also compare the experimental results with Barracuda simulations. The performance of Barracuda for accurate predictions of bed pressure drop and the minimum fluidization velocity was studied. The computational model, model development and the information about the geometry were also included there. Chladek et al. (36) explains the possibility of using fluidization as a technique to separate a particle mixture with different size and density. This is the basis for the design of the novel classification system.

Case specific CFD model with Barracuda® is made based on the knowledge gain from the simulations done on the cylindrical fluidized bed. A details investigation is done for selecting a suitable drag model for the crossflow solid classifier CFD modelling and reported in a separate article which is currently under review (44). Further CFD studies are done on the cold flow solid classification with classifier version 5.1v and findings are discussed in Jayarathna et al. (40).

5. Scaling between cold-flow lab-scale and hot-flow pilot-scale conditions

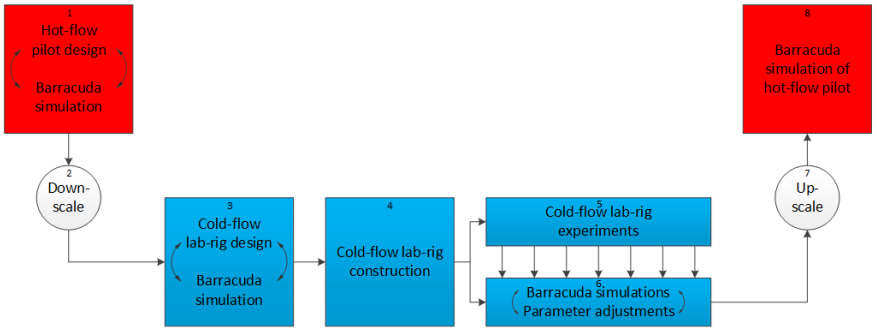

Fig. 10. The work procedure followed during the PhD research work regarding the novel solid classifier design

Investigation of the cold-flow classification system to predict performance of the hot flow system required scaling calculations. Fig. 10, illustrates the work procedure followed during the current research work. The size of the down-scaled cold-flow lab-rig geometry (box no. 3 in Fig. 10) was based on the existing air supply fan and size considerations. The idea was to make the unit which is practical to build (not miniature) and easy to operate with existing equipment (not too large).

5.1. Dimensionless numbers used in scaling

Scaling model is shown from equation 1 to 6. Down-scaling or up-scaling is typically done by making sure that the key dimensionless numbers which characterize the process are kept at (almost) the same values in both systems. For a system involving fluidization and entrainment of particles by a gas, one may require that the following dimensionless numbers are kept constant (45):

- Particle Reynolds number (same ratio of inertia forces / friction forces), Re_p
- Froude number (same ratio of inertia forces / gravity forces), Fr
- Gas Reynolds number (same turbulence level in the gas phase), Re
- Particle/gas density ratio, R
- Particle/gas mass flux ratio, M
- Height/hydraulic diameter ratio, S
- Particle size distribution, PSD
- Particle sphericity, φ

$$Re_p = \frac{\rho u_0 d_p}{\mu} \quad (1)$$

$$Fr = \frac{u_0}{\sqrt{g D_h}} \quad (2)$$

$$Re_D = \frac{\rho u_0 D_h}{\mu} \quad (3)$$

$$R = \frac{\rho_p}{\rho} \quad (4)$$

$$M = \frac{G}{\rho u_0} \quad (5)$$

$$S = \frac{L}{D_h} \quad (6)$$

Here, ρ is gas density [kg/m³], u0 is superficial gas velocity [m/s], dp is particle size [m], μ is dynamic gas viscosity [Pa·s], g is the gravity constant [m/s²], Dh is hydraulic diameter of the classifier [m], ρp is particle density [kg/m³] and G is the gas mass flux in the classifier [kg/(s·m²)].

5.2. Hot-flow pilot-scale and cold-flow lab-scale conditions

Requiring all dimensionless numbers to be the same in two systems may not always be possible. A key factor in this connection is the operational temperature in the two systems. A big difference in temperature (20 vs 910 °C) gives a big difference in dynamic viscosity and gas density, and hence in kinematic viscosity ($\nu \equiv \mu/\rho$), for a given gas. The gas and particle characteristics in the hot-flow pilot-scale system was usually given, so the characteristics at cold-flow lab-scale conditions must be adapted. But particles of the right size (and PSD and sphericity) and gases with the right properties may not be readily available. Furthermore, space constraints may prevent the use of the optimum size of the cold-flow geometry.

In the current research project, the specifications used for hot-flow conditions are shown in Table 1.

Table 1. Specifications for hot-flow conditions

Specification	Gas/Values
Fluidization gas	CO2
Operating temperature	910 °C
Operating pressure	≈ 1 atm
Sorbent (CaCO3) particle size (mean)	175 µm
HT particle size (mean)	1000 µm
Equivalent power plant size	300kW

Due to lab constraints, ambient air was used (20 °C; 1 atm) as the fluidization gas at cold-flow conditions, and the size of the cold-flow unit was constrained by the availability of compressed air (volume flow rate range).

As a consequence of these constraints, the size of the cold-flow unit could not be matched to the size of the hot-flow unit, hence the gas Reynolds number is not the same in the two systems. Table 2 gives an overview of the key values for the two systems.

Table 2. Summary of hot-flow and cold-flow characteristics

Property	Unit	Hot-flow pilot-scale	Cold-flow lab-scale, optimum	Cold-flow lab-scale, actual
Gas	-	CO_2	-	Air
Sorbent	-	CaO	-	Zirconium silicate
HT solids	-	$Al2O_3$	-	Steel
Temperature	°C	910	-	20
Pressure	atm	1	-	1
Gas molecular mass	kg/mol	0.044	-	0.029
Gas density	kg/m³	0.47	-	1.21
Kinematic viscosity	m²/s	9.5·10-5	-	1.5·10-5
Sorbent envelope density	kg/m³	1760	4591	3800
HT-solids envelope density	kg/m³	3000	7825	7800
Mean sorbent particle size	µm	175	51	69
Mean HT particle size	µm	1000	289	290
Sorbent settling velocity	m/s	0.59	0.32	0.27
HT solids settling velocity	m/s	8.7	4.7	3.95
Superficial gas velocity	m/s	4.7	2.5	0.7-2.3[c]
Classifier length	mm	529	153/216	350
Classifier width	mm	75	22	50
Solids loading	kg/kg	7.1	7.1	5-90[c]
Sorbent weight fraction	kg/kg	0.28	0.28	0.28
Sorbent/gas ratio	kg/kg	2	2	1-25[c]
Gas flow rate	kg/h	311	37	51-174[c]
Sorbent flow rate	kg/h	623	73	217-1555[c]
HT solids flow rate	kg/h	1598	188	557-3999[c]
Sorbent mass flux	kg/(m²s)	4.3	6.1	3-25[c]
Sorbent/gas density	-	3783	3783	3131
Sorbent Reynolds number	-	1.1	1.1	2.2
HT solids Reynolds number	-	92	92	92
HT-solids/gas density	-	6447	6447	6427
Classifier Reynolds number	-	6486	6486	15256
Sorbent/gas mass flux ratio	-	2	2	1.2-26[c]
Froude number	-	4.1	4.1	2.8
Equivalent power plant size	kW	300	300	892-6390[c]

[c] Variable range in the lab-rig

The envelope density of the cold-flow sorbent is somewhat lower than the optimum value due to particle availability constraints, but the difference is not very big, so should be ok. The HT particle envelope density is very close to the target value. The particle sizes at cold-flow conditions also match the target values quite well. Based on this, the settling velocities and the particle Reynolds numbers are not very different from the target values. The optimum gas flow rate at cold-flow conditions is quite well covered by the range of the lab classifier. All this suggests that the particle hydrodynamics will be quite similar in the two systems.

The lab-scale classifier is, however, about twice as big as the optimum cold-flow classifier. This is due to size constraints (operating a very small classifier in the lab may be difficult) and air supply constraints, as previously mentioned. And also, the solids feed rate range of the lab classifier is significantly higher than the target value. This means that the equivalent power plant duty is significantly higher than the targeted 300 kW.

6. CFD simulation of the hot-flow pilot-scale classifier

The purpose of running CFD simulations in a hot-flow pilot-scale unit is to determine the classification efficiency under these conditions and thereby reduce the risk of building a pilot which may not work properly. Upscaling from the cold-flow lab-scale unit to a hot-flow pilot-scale unit, applying the procedure described in section 5, however results in a classifier size corresponding to an 892-6390 kW, i.e. 3-21 times bigger than the targeted 300 kW size. (As explained in section 6, this is due to the practical laboratory constraints.)

Since upscaling to 300 kW cannot be done properly based on the existing lab-rig, the lab-scale geometry is here re-used also at hot-flow conditions (i.e. no scaling of the geometry). However, the particle densities and sizes are scaled to match with a temperature of 910 °C, as explained. Depending on what flow rates that are applied, the current geometry may cover a quite wide range of equivalent thermal power, see Table 3.

Table 3. Operational settings for applying the lab-scale geometry 5.1 unit at hot-flow conditions.

Parameters	**Unit**	**300kw**	**109kw**	**50kw**
Terminal Settling velocity of sorbent at hot flow	m/s	0.6	0.6	0.6
Terminal Settling velocity of HT particles at hot flow	m/s	8.5	8.5	8.5
Superficial gas velocity at hot flow conditions	m/s	4.55	5.17	4.55
Cross sectional area of the 5.1v classifier	m2	0.0175	0.0175	0.0175
Gas volume flow rate at hot flow conditions	m3/s	0.0796	0.0905	0.0796
Gas density at hot flow conditions	kg/m3	0.453	0.453	0.453
Gas mass flow rate at hot flow conditions	kg/s	0.036	0.041	0.036
Gas mass flow rate at hot flow conditions	kg/h	130	148	130
Thermal power of the coal-fired power plant	kW	300	109	50
Heating value of coal	MJ/kg	27.7	27.7	27.7
Mass flow rate of coal	kg/s	0.011	0.004	0.002
Mass flow rate of coal	kg/h	39	14	6
CO2/Coal mass ratio	kg/kg	2.6	2.6	2.6
CO2 generated	kg/s	0.028	0.010	0.005
CO2 generated	kg/h	101	37	17
CO2 capture ratio	-	85%	85%	85%
CO2 captured	kg/s	0.024	0.009	0.004
CO2 captured	kg/h	86	31	14
Stoichiometric CaO required to capture the CO2	kg/s	0.030	0.011	0.005
Stoichiometric CaO required to capture the CO2	kg/h	110	40	18
Activity of the sorbent	-	18%	18%	18%
Actual CaO (sorbent) required to capture the CO2	kg/s	0.169	0.062	0.028
Actual CaO (sorbent) required to capture the CO2	kg/h	609	222	102
Sorbent mass fraction in the particle mixture	-	28%	28%	28%
Solid flow rate	kg/s	0.6	0.22	0.10
Solid flow rate	kg/h	2176	792	363
Solids loading	kg/kg	16.7	5.4	2.8
Sorbent loading	kg/kg	4.7	1.5	0.8

6.1. Case definition and simulations inputs

The settling velocities of sorbent and HT-solids are 0.6 and 8.5 m/s, respectively. Hence, the superficial gas velocity should be between those two values. Two different cases have been simulated to try to determine the optimum velocity. All the other parameters than the gas velocity is kept constant (as given in Table 2 and Table 3).

Hot flow simulations are done with a mixture of alumina and CaO particles. The particle properties are shown in Table 2 under the "hot flow pilot". CO_2 is used as the fluidization gas, and the simulation is done at 910 °C (see Table

1). Simulations are done with Barracuda, and the model is explained in Jayarathna et al.(38) and Jayarathna et al. (44). According to the Geldart classification, alumina and CaO particles can be categorized as D and B particles, respectively. According to the study in Amarasinghe et al. (37), using the Wen-Yu/Ergun blended drag model and with some coefficient as explained in Jayarathna et al.(38).

The same 5.1v geometry and the mesh from the cold-flow simulations were used for the hot flow simulations and the gas velocities used for each of the chambers in the classifier are shown in Table 4.

Table 4. 109 kW cases simulated with different superficial gas velocities

Case	Superficial gas velocity [m/s]						S/G
	Ch. 1	Ch. 2	Ch. 3	Ch. 4	Ch. 5	Ave	
A	2.7	2.4	3.5	4.9	5.2	3.5	7.9
B	1.6	1.4	2.1	2.9	3.1	2.1	13.2

6.2. Case A: Average superficial gas velocity 3.5 m/s

A case corresponding to 109 kW (see Table 3) has been simulated with an average gas flow velocity of 3.5m/s. Preliminary results after pseudo steady state is achieved is shown in Fig. 11 to Fig. 14. The sorbent (CaO) bottom exit loss is zero, but the HT-solids (alumina) top exit loss is 5.1 %. This suggests that the superficial gas velocity is higher than the required rate and one could achieve a better classification with a lower superficial gas flow rate. With a lower velocity, the HT-solids top exit loss will be reduced, and most likely the sorbent bottom exit loss can still be kept very low.

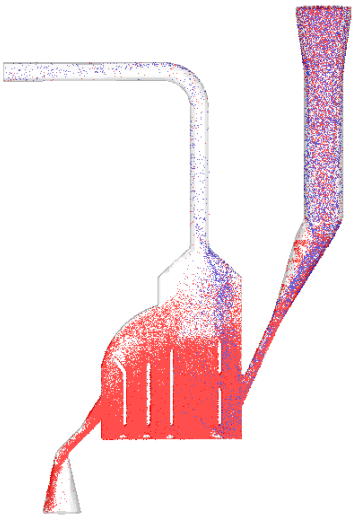

Fig. 11. Snapshot of sorbent (blue) and HT-solids (red) distribution in geometry 5.1 operating under hot-flow conditions, with gas velocity 3.5 m/s, after 60 seconds

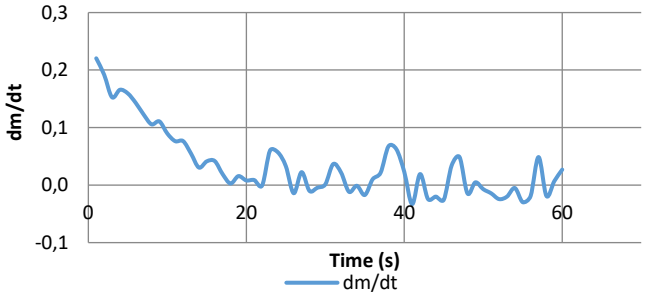

Fig. 12. Accumulation of mass in classifier geometry 5.1 at hot-flow conditions, with gas velocity 3.5 m/s

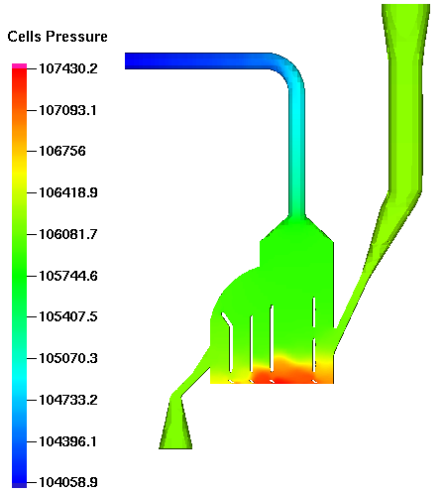

Fig. 13. Pressure distribution in classifier geometry 5.1 after 60 seconds for the case with gas velocity 3.5 m/s

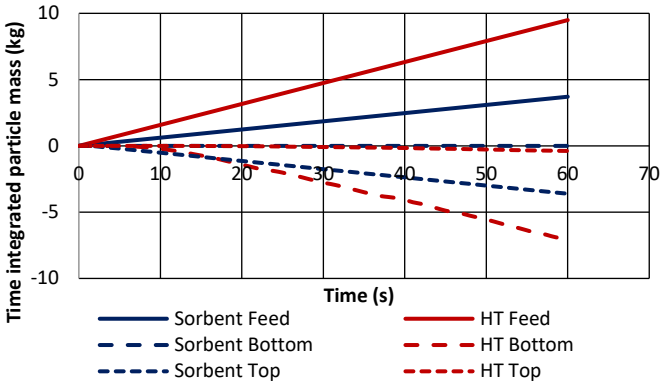

Fig. 14. Input and output streams for the case with gas velocity 3.5 m/s

According to the graphical representation of the particle distribution inside the classifier in Fig. 12, most of the sorbent particle (in blue) leave the classifier while passing through the first two compartments. This is also a sign of too high superficial gas velocity.

Fig. 13, shows the input (positive) and output (negative) streams of solids for the case with gas velocity 3.5 m/s. It is seen that all the sorbent in the feed is leaving from the top exit and there are no sorbent particles in the bottom exit. However, a small fraction of HT solid particles is leaving from the top outlet while most of them are leaving from the bottom outlet.

Fig. 14, shows the pressure distribution inside the classifier. Highest pressure is predicted in the first three compartments (from right side) where the particle bed is higher.

6.3. Case B: Average superficial gas velocity 2.1 m/s

The case corresponding to 109 kW has been simulated with an average gas flow velocity of 2.1 m/s. Results (pseudo steady state) are shown in Fig. 15 to Fig. 18. The sorbent (CaO) bottom exit loss is still close to zero (0.01%), and now the HT-solids (alumina) top exit loss has dropped to 0.4 %.

This suggests that the superficial gas velocity is now in the proper range.

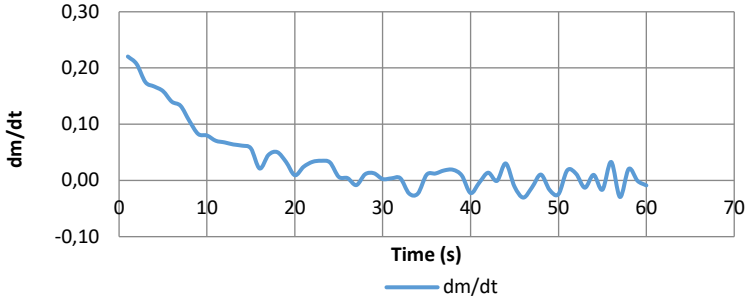

Fig. 16. Accumulation of mass in classifier geometry 5.1 at hot-flow conditions, with gas velocity 2.1 m/s

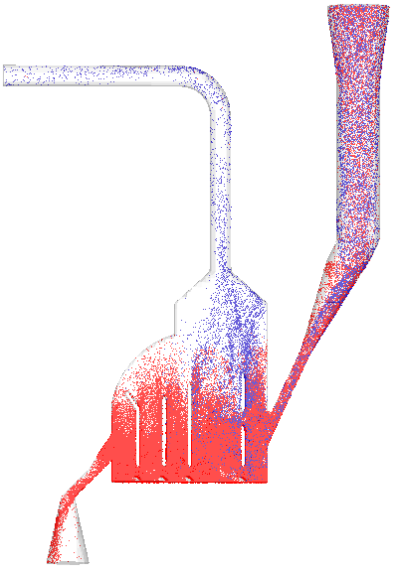

Fig. 15. Snapshot of sorbent (blue) and HT-solids (red) distribution in geometry 5.1 operating under hot-flow conditions, with gas velocity 2.1 m/s, after 60 seconds

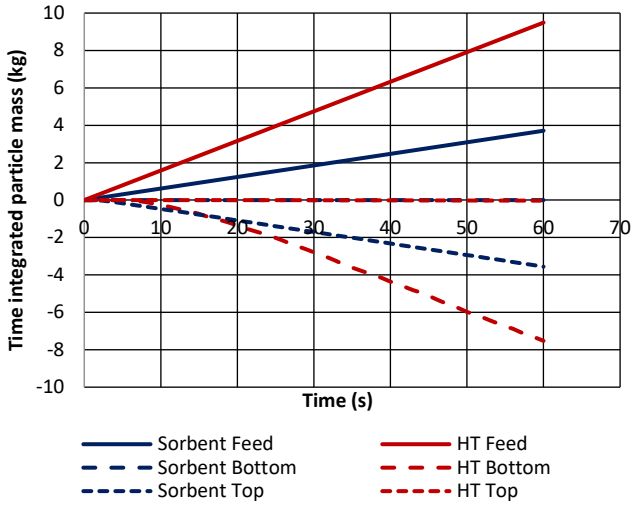

Fig. 17. Input and output streams for the case with gas velocity 2.1 m/s

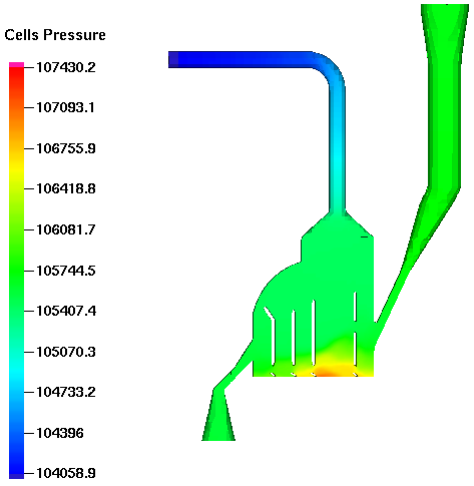

Fig. 18. Pressure distribution in classifier geometry 5.1 after 60 seconds for the case with gas velocity 2.1 m/s

6.4. Evaluation of the case study

Fig. 12 and Fig. 16 show the sorbent (blue) and HT solids (red) behavior inside the classifier in Case A and Case B respectively. The thickness of the dense particle bed is higher in case A compared to case B due to the higher superficial air velocity, and that explains the poor classification efficiency in case A.

Barracuda simulation have shown that the classifier reaches the pseudo steady state within 40 seconds in both cases. This is visualized from the variation of the accumulated mass inside the classifier with the time shown in Fig. 11 (for case A) and Fig. 15 (for case B).

The high pressure shown at the bottom of the classifier in case A is bigger (see Fig. 14 and Fig. 18) compared to the high-pressure zone in Case B. Higher air flow rates create higher drag on particles and their reverse effect on air flow create a larger high-pressure zone at the bottom of the classifier.

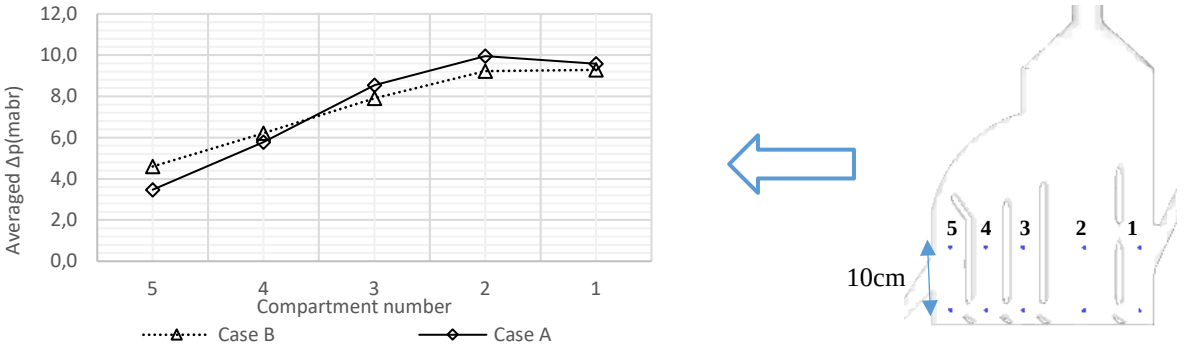

Fig. 19. Average pressure drop in each compartment in the 5.1v classifier for case A and case B

Fig. 19 shows the average pressure drop in each compartment for case A and case B. Average pressure drop is recorded in between the transient points shown in the classifier sketch Fig. 19. The bottom transient points are located 2.5cm above the bottom wall of the classifier and the distance between the transient points in each compartment is 10cm. Each of the average pressure recording points in the graph represent the static pressure of the particle bed in each compartment. The shape of the average pressure curves explains that Case A has a higher particle mass than Case B in the first three compartments.

There is a higher superficial velocity in compartments in Case A compared to case B and this probably cause for early classification (within first 3 compartments) of particles in Case A. Because of that Case A gets rid of a large portion of particles before the particles reach compartments 4 and 5. As a result of that the particle concentration in those compartments are lower compared to case B. This can be the reason for lower pressure drop in last two compartments in Case A.

It has been shown in previous experiments and Barracuda simulations that the current geometry (5.1v) gives a relatively good classification of steel particles (d_{50}= 290 µm) and zirconia particles (d_{50}= 70 µm) at cold-flow conditions. These particle sizes correspond to calcium oxide (sorbent) and alumina (HT-solids) sizes of approximately 175 and 1000 µm at hot-flow conditions.

According to the original project goal, a hot-flow pilot of 300 kW should be designed. The current cold-flow geometry is however equivalent to a hot-flow pilot in the order of 900-6000 kW (depending on operating conditions) if scale-up rules are applied. Partly this is due to practical laboratory constraints, such as fluidization gas availability, fan size and practical rig size considerations, all applied to facilitate construction and operation.

Instead of scaling-up the geometry size, Barracuda has been used to simulate the current geometry under hot-flow conditions, i.e. at 910 °C and applying sorbent and HT particle sizes of 175 and 1000 µm, respectively. The simulation results indicate that the classifier will work well also at hot-flow conditions, although more simulations would be necessary to pinpoint the best setpoint for the flow rates.

Simulating the hot flow classifier for a size for pilot plant with 109 kw capacity proved that the classifier is function well at hot flow conditions with 13% solids loading value which is higher that the solid loading achieved for the best case with the cold flow experiments and simulations (7%).

According to the original project goal, a hot-flow pilot of 300 kW should be designed. The current cold-flow geometry is however equivalent to hot-flow pilot in the order of 900-6000 kW (depending on operating conditions) if scale-up rules are applied. Partly this is due to practical laboratory constraints, such as fluidization gas availability, fan size and practical rig size considerations, all applied to facilitate construction and operation.

Instead of scaling-up the geometry size, Barracuda® has been used to simulate the current geometry under hot-flow conditions, i.e. at 910 °C and applying sorbent and HT particle sizes of 175 and 1000 µm, respectively. The simulation results indicate that the classifier will work well also at hot-flow conditions, although more simulations would be necessary to pinpoint the best setpoint for the flow rates.

7. Overall conclusion

This chapter gives and overall conclusion of the current research work, which was functioning as 4 years of research work. Scientific finding from the current research work is previously published with nine (21, 27, 31, 35-38, 40, 44) different publications. FICaL can be categorized as an attractive technology with a low energy penalty when applied to a coal-fired power plant. Various concepts of indirect heat transfer were studied and evaluated through process simulations with Aspen Plus. Based on these studies, FICaL can be categorized as a competitive technology with a low energy penalty. A simplified method was used to estimate energy penalties in the order of 1 %.

The present stage of the fully integrated calcium looping (FICaL) technology was evaluated. FICaL can be categorized as an attractive technology, with a low energy penalty when applied to a coal-fired power plant. Various concepts of indirect heat transfer were studied and evaluated through process simulations with Aspen Plus. Based on these studies, FICaL can be categorized as a competitive technology with a low energy penalty. A simplified method was used to estimate energy penalties in the order of 1 %.

Using inert heat transfer (HT) particles to transfer the heat was selected as the best option to implement indirect heat transfer. In this concept, the HT particles are first heated by direct heat transfer in the combustor, and then heat is transferred from the HT particles to the sorbent in the calciner to provide the calcination heat.

A novel cross-flow fluidized bed classifier was designed, using CFD as a supporting tool, in order to separate the sorbent and HT particles exiting from the calciner. The classifier, which has no mechanical moving parts exposed to very high temperature, can be operated under the required high-temperature conditions prevailing in a full-scale plant.

Two different cold-flow lab-scale versions of the classifier was built and used in a huge number of experiments. The second and improved version was able to classify very well a mixture of down-scaled sorbent particles (zirconia) and down-scaled HT particles (steel or bronze). In the classification, the aim is to minimize the loss of sorbent particles via the bottom exit from the classifier, and also minimize the loss of HT particles via the top exit from the classifier. The experiments with the improved classifier version gave particle losses in the order of 2-3 %, and these values are very close to what considered as acceptable in a full-scale hot-flow system.

Extensive CFD simulations were carried out with the commercial software Barracuda to investigate in detail how different particle types behave in the classifier. Even if the exact particle losses were not well predicted, Barracuda is able to predict the general gas-solids flow behavior and proved to be a useful tool in the design and improvement of the classifier, and also in interpretation of the experimental results. Barracuda was also used to simulate the classification process under hot-flow conditions, and indicated that the classifier will also perform well under these conditions.

The iterative design and modelling effort from this research work has produced a functional, high-efficiency classification concept.

Reference

1. Choices AsC. Environmental Effects of Increased Atmospheric Carbon Dioxide. 2011;The National Academies Press.(ISBN 978-0-309-14585-5):15.
2. Robinson AB, Robinson NE, Soon W. Environmental Effects of Increased Atmospheric Carbon Dioxide. Journal of American Physicians and Surgeons. 2007;12(3):79-90.
3. McGee M. Global Carbon Emissions: CO2.earth, A Pro Oxygen Website; 2017 [cited 2017 04/05/2017]. Available from: https://www.co2.earth/global-co2-emissions.
4. UNFCCC. Kyoto Protocol to the United Nations Framework Convention on Climate Change. Review of European Community & International Environmental Law. 1998;7(2):214-7.
5. UNFCCC. Adoption of the Paris agreement 2015 [cited 2015 15/12]. FCCC/CP/2015/l.9/Rev.1:[Available from:

http://unfccc.int/resource/docs/2015/cop21/eng/l09r01.pdf.
6. Petrescu L, Bonalumi D, Valenti G, Cormos A-M, Cormos C-C. Life Cycle Assessment for supercritical pulverized coal power plants with post-combustion carbon capture and storage. Journal of Cleaner Production. 2017;157:10-21.
7. Gorset O, Knudsen JN, Bade OM, Askestad I. Results from Testing of Aker Solutions Advanced Amine Solvents at CO2 Technology Centre Mongstad. Energy Procedia. 2014;63:6267-80.
8. Desideri U. 5 - Advanced absorption processes and technology for carbon dioxide (CO2) capture in power plants A2 - Maroto-Valer, M. Mercedes. Developments and Innovation in Carbon Dioxide (CO2) Capture and Storage Technology. 1: Woodhead Publishing; 2010. p. 155-82.
9. Erans M, Manovic V, Anthony EJ. Calcium looping sorbents for CO2 capture. Applied Energy. 2016;180:722-42.
10. Hanak DP, Biliyok C, Anthony E, Manovic V. Evaluation of a calcium looping CO2 capture plant retrofit to a coal-fired power plant. Computer Aided Chemical Engineering. 2016;38:2115-20.
11. Shimizu T, Hirama T, Hosoda H, Kitano K, Inagaki M, Tejima K. A Twin Fluid-Bed Reactor for Removal of CO2 from Combustion Processes. Chemical Engineering Research and Design. 1999;77(1):62-8.
12. Lasheras A, Ströhle J, Galloy A, Epple B. Carbonate looping process simulation using a 1D fluidized bed model for the carbonator. International Journal of Greenhouse Gas Control. 2011;5(4):686-93.
13. Chang MH, Huang CM, Liu WH, Chen WC, Cheng JY, Chen W, et al. Design and Experimental Investigation of Calcium Looping Process for 3-kWth and 1.9-MWth Facilities. Chemical Engineering & Technology. 2013;36(9):1525-32.
14. Ströhle J, Junk M, Kremer J, Galloy A, Epple B. Carbonate looping experiments in a 1 MWth pilot plant and model validation. Fuel. 2014;127(0):13-22.
15. Dieter H, Bidwe AR, Varela-Duelli G, Charitos A, Hawthorne C, Scheffknecht G. Development of the calcium looping CO2 capture technology from lab to pilot scale at IFK, University of Stuttgart. Fuel. 2014;127(0):23-37.
16. Kremer J, Galloy A, Ströhle J, Epple B. Continuous CO2 Capture in a 1-MWth Carbonate Looping Pilot Plant. Chemical Engineering & Technology. 2013;36(9):1518-24.
17. Chang M-H, Chen W-C, Huang C-M, Liu W-H, Chou Y-C, Chang W-C, et al. Design and Experimental Testing of a 1.9MWth Calcium Looping Pilot Plant. Energy Procedia. 2014;63:2100-8.
18. Martínez A, Lara Y, Lisbona P, Romeo LM. Energy penalty reduction in the calcium looping cycle. International Journal of Greenhouse Gas Control. 2012;7:74-81.
19. Strelow M, Schlitzberger C, Röder F, Magda S, Leithner R. CO2 Separation by Carbonate Looping Including Additional Power Generation with a CO2-H2O Steam Turbine. Chemical Engineering & Technology. 2012;35(3):431-9.
20. Alstom. Fully Integrated Regenerative Carbonate Cycle (FIRCC), Pre-study description. Alstom; 2012 18th October.
21. Jayarathna CK, Halvorsen BM, Tokheim L-A. Experimental and Theoretical Study of Minimum Fluidization Velocity and Void Fraction of a Limestone Based CO2 Sorbent. Energy Procedia. 2014;63(0):1432-45.
22. Junk M, Reitz M, Ströhle J, Epple B. Thermodynamic evaluation and cold flow model testing of an indirectly heated carbonate looping process. 2nd International Conference on Chemical Looping, Darmstadt, Germany; 26-28 September2012.
23. Junk M, Reitz M, Ströhle J, Epple B. Thermodynamic Evaluation and Cold Flow Model Testing of an Indirectly Heated Carbonate Looping Process. Chemical Engineering & Technology. 2013;36(9):1479-87.
24. Hoeftberger D, Karl J. Self-Fluidization in an Indirectly Heated Calciner. Chemical Engineering & Technology. 2013;36(9):1533-8.
25. Reitz M, Junk M, Ströhle J, Epple B. Design and Erection of a 300 kWth Indirectly Heated Carbonate Looping Test Facility. Energy Procedia. 2014;63:2170-7.
26. Junk M, Kremer J, Ströhle J, Eimer N, Priesmeier U, Weingärtner C, et al. Design of a 20 MWth Carbonate Looping Pilot Plant for CO2-capture of Coal Fired Power Plants by Means of Limestone. Energy Procedia. 2014;63:2178-89.
27. Jayarathna CK, Mathisen A, Øi LE, Tokheim L-A. Process Simulation of Calcium Looping with Indirect Calciner Heat Transfer. SIMS 56; October 7–8, 2015; Linkoping, Sweden. Proceedings of SIMS 56,2015.
28. Abanades JC, Anthony EJ, Wang J, Oakey JE. Fluidized Bed Combustion Systems Integrating CO2 Capture with CaO. Environmental Science & Technology. 2005;39(8):2861-6.
29. Abanades JC, Oakey JE, Alvarez D, Hämäläinen J. Novel Combustion Cycles Incorporating Capture of CO2 with CaO. Greenhouse Gas Control Technologies - 6th International Conference. Oxford: Pergamon; 2003. p. 181-6.
30. Abanades JC, Oakey JE, inventorsCombustion method with integrated CO2 separation by means of carbonation. United States patent US 2005OO60985A1. 2002 24/03/2005.
31. Jayarathna CK, Mathisen A, Øi LE, Tokheim L-A. Aspen Plus® Process Simulation of Calcium Looping with Different Indirect Calciner Heat Transfer Concepts. Energy Procedia. 2017;114:201-10.
32. Glicksman LR. Scaling relationships for fluidized beds. Chemical Engineering Science. 1984;39(9):1373-9.
33. Glicksman LR. Scaling relationships for fluidized beds. Chemical Engineering Science. 1988;43(6):1419-21.
34. Glicksman LR, Hyre M, Woloshun K. Simplified scaling relationships for fluidized beds. Powder Technology. 1993;77(2):177-99.
35. Jayarathna CK, Chladek J, Balfe M, Moldestad BME, Tokheim L-A. Impact of solids loading and mixture composition on the classification efficiency of a novel cross-flow fluidized bed classifier. Powder Technology. 2018;336:30-44.
36. Chladek J, Jayarathna CK, Moldestad BME, Tokheim L-A. Fluidized bed classification of particles of different size and density. Chemical Engineering Science. 2018;177:151-62.
37. Amarasinghe WS, Jayarathna CK, Ahangama BS, Moldestad BME, Tokheim L-A. Experimental study and CFD modelling of fluidization velocity for Geldart A, B and D particles. International Journal of Modeling and Optimization. 2017;7(3).
38. Jayarathna CK, Moldestad BME, Tokheim LA, editors. Validation of results from Barracuda® CFD modelling to predict minimum fluidization velocity and pressure drop of Geldart A particles. SIMS 58; 2017 September 25-27 2017; Reykjavik, Iceland2017.
39. Kunii DLO. Fluidization engineering. Boston,Mass.: Butterworths; 1991.
40. Jayarathna CK, Balfe M, Moldestad BME, Tokheim L-A. Improved multi-stage cross-flow fluidized bed classifier. Powder Technology. 2019;342:621-9.
41. Snider DM. An Incompressible Three-Dimensional Multiphase Particle-in-Cell Model for Dense Particle Flows. Journal of Computational

Physics. 2001;170(2):523-49.
42. Andrews MJ, O'Rourke PJ. The multiphase particle-in-cell (MP-PIC) method for dense particulate flows. International Journal of Multiphase Flow. 1996;22(2):379-402.
43. Snider DM, Clark SM, O'Rourke PJ. Eulerian–Lagrangian method for three-dimensional thermal reacting flow with application to coal gasifiers. Chemical Engineering Science. 2011;66(6):1285-95.
44. Jayarathna CK, Balfe M, Moldestad BME, Tokheim LA. Comparison of experimental results from operating a novel fluidized bed classifier with CFD simulation results applying seven different drag models. International Journal of Chemical Engineering. 2021;Submitted.
45. Markström P, Lyngfelt A. Designing and operating a cold-flow model of a 100 kW chemical-looping combustor. Powder Technology. 2012;222:182-92.